Journal of Nuclear Research and Applications

Research Paper

Vol. 2, No. 4, Autumn (2022), P 7-14

Cited in: https://jonra.nstri.ir

Received: 18 March 2022, Accepted: 13 June 2022

Investigation of Feed Flow Effect Using CFD-DSMC Method in a Gas Centrifuge

V. Ghazanfari*, M. M. Shadman, F. Mansourzadeh

Nuclear Fuel Cycle Research School, Nuclear Science and Technology Research Institute (NSTRI), P.O. Box:11365-8486, Tehran, Iran

ABSTRACT

In this study, the effect of the rarefied region in the centrifuge rotor was investigated. In a centrifuge rotor, the feed inlet is positioned in the rarefied area. The continuum hypothesis is not valid in the rarefied area; therefore, it desires to be analyzed by probabilistic methods like Direct Simulation Monte Carlo (DSMC). The present study uses the Computational Fluid Dynamic (CFD) method to simulate the continuum area, and the DSMC method is employed in the rarefied area. An implicit coupled density-based scheme was performed for the CFD method, and Variable Hard Sphere (VHS) and diffuse models were employed in the DSMC method. Also, the local Knudsen number was defined to determine the interface location between the continuum-rarefied regions (r=0.086 m). The comparison results of pure CFD and CFD-DSMC methods illustrated large differences between the flow properties in the rarefied regions. The results showed that the value of separation power obtained from pure CFD and CFD-DSMC solution is 10.5% different.

***Keywords*:** Feed flow, Gas centrifuge, CFD-DSMC, Separation

I. Introductions

The gas flow regime inside the rotor covers the total range from free molecular (near the axis) to the continuum (near the rotor wall). CFD is employed to analyze the continuum region, and DSMC is one of the best methods for flow analysis in the rarefied region. So the analysis of gas flow fields in the rotor desires progressive methods such as a coupled CFD-DSMC. Numerous studies in analysis flow, including rarefied and continuum areas, have used hybrid CFD-DSMC methods, e.g., a supersonic flow over a quasi-2-D wedge [1], and a hypersonic flow over a 2-D cylinder [2]. So far, many studies have been performed to analyze the gas flow inside the rotor, in which the continuum area inside the rotor is simulated, while the rarefied area is not accurately modeled [3,4].

Zeng et al. examined the simulation of the gas flow inside the centrifuge using a computational fluid dynamics (CFD) method. They used the finite volume method and upwind implicit second-order equation to solve Navier-Stokes equations [5]. Bogovalov et al. simulated the gas flow inside a centrifuge rotor and the separation of isotopes in an axisymmetric state using numerical and semi-analytical methods [6].

Jiang et al. employed a 3-D model to simulate the flow structures of a feed jet in a rotating flow field

**Corresponding Author name*: V. Ghazanfari
E-mail address: vali.ghazanfari@gmail.com

using a CFD code. It was demonstrated that because of the vacuum regime in the region near the axis of rotation, the results of a CFD code numerical simulation ring errors [7]. Recently, Ghazanfari et al. developed a CFD solver to simulate the UF_6 gas flow in the centrifuge's rotor. An Implicit Coupled Density-Based (ICDB) solver, based on the AUSM +up scheme, was developed in OpenFOAM. The thermal and mechanical drives were considered simultaneously in the rotor. It was revealed that all uranium gas flow characteristics, including velocity, pressure, temperature, axial mass flux, and uranium isotope separation parameters, including separation power and separation coefficients, could well be predicted [8].

This study investigates the effect of feed flow using the CFD-DSMC method in a gas centrifuge. The radial velocity obtained from CFD and DSMC methods is compared in the feed zone. Finally, the consequence of rarefied areas on separation efficiency is evaluated.

II. RESEARCH THEORIES

The UF_6 gas flow in the rotor is governed by a full set of hydrodynamic equations, including the conservation laws of mass, momentum, and energy [9]:

$$\nabla,(\rho V) = 0 \tag{1}$$

$$\nabla,(\rho VV) = -\nabla p + \nabla,\tau \tag{2}$$

$$\nabla,(\rho Ve) = -\nabla,(k\nabla T) - \nabla,(pV) + \nabla,(\tau,V) \tag{3}$$

The equation of state for an ideal gas is $p/\rho = \frac{R}{M}T$

M is the molar mass of the considered gas, R is the universal gas constant, and T is the temperature. Also, V is the velocity vector, ρ is the density, p is the pressure, e is the specific total energy, and τ is the stress tensor.

To calculate the separation power, it is necessary to find the concentration distribution in the centrifuge's rotor. For this purpose, the convection-diffusion equation is solved [9].

The convection-diffusion equation of component A is employed as follows [10]:

(4)

$$\nabla,[(-\rho D_{AB})\nabla x_A] + \frac{\Delta M}{R}\nabla,$$

$$\left[(-\rho D_{AB})\left(\frac{x_A(1-x_A)}{\rho T}\nabla p\right)\right] +$$

$$\nabla,[(-\rho D_{AB})(k_T\nabla \ln T)] + \nabla,\left(\rho x_A\vec{V}\right) = 0$$

Where, x_A is the molar fraction of isotope A, D_{AB} is the diffusion coefficient of isotope A in isotope B, k_T is the thermal diffusion ratio, ΔM is the difference between the light and heavy isotope molecular mass.

The separation of power is as follows [9]:

$$\delta U = P(2y_P - 1)ln\frac{y_P}{1-y_P} + W(2x_W - 1)ln\frac{x_W}{1-x_W} - F(2z_F - 1)ln\frac{z_F}{1-z_F} \tag{5}$$

Where W, P, and F are the flow rate of the tailed, enriched, and feed flow in the separation unit, respectively. z_F, y_P, and x_W signify the molar concentration of feed, product, and waste, respectively.

To solve the hydrodynamic equations using the CFD method, we used an Implicit Coupled Density-Based solver that has been created in the OpenFOAM framework. In the DSMC method, the gas flow is studied at the molecular level. The flow's macroscopic properties, including temperature, pressure, and velocity, are obtained using particle velocity. In this study, the dsmcFoam solver was utilized in OpenFOAM to analyze the rarefied areas. In dsmcFoam solver, the wall interaction and binary collision models were selected based on the Diffuse model and Larsen-Borgnake Variable Hard Sphere model, respectively [6].

III. Fundamental equations in the rarefied region

DSMC is a random and particle-based method used to calculate and analyze rarefied gas flows [11]. This is a relatively new numerical model introduced in 1963 [12]. However, this method has become one of the preferred methods for simulating non-equilibrium gas flows, which should consider the molecular nature of the gas [13].

In the DSMC method, the gas flow is studied at the molecular level. The flow's macroscopic properties, including temperature, pressure, and velocity, are obtained using particle velocity.

The DSMC method consists of 5 steps. 1- Initialization 2- Particle motion 3- Indexing 4- Particle collision with each other and walls 5- Extraction of macroscopic quantities. This method uses many model molecules to simulate real molecules, which are far fewer in number than real molecules. Therefore, each model molecule represents a large number of real molecules.

Good DSMC performance dictates that cells contain at least 20 compute particles. Also, the simulation time-step should be less than the minimum average collision time and average residence time. Furthermore, cell size should be small compared to the mean free path [14].

In this study, the dsmcFoam solver was utilized in OpenFOAM to analyze the rarefied areas. In dsmcFoam solver, the wall interaction model and binary collision model were selected based on the Diffuse model and Variable Hard Sphere, respectively. The number of cells in the rarefied region was 110000. The number of particles per cell was considered 20.

IV. CFD-DSMC procedure

In a hybrid procedure, one crucial question is determining the interface between two regions. The Gradient Length Local Knudsen number suggested by Wang and Boyd has been used in our study to illustrate the breakdown of the continuum hypothesis [15]. The second point is how to transfer the characteristic of the flow (including pressure, velocity, and temperature) between these two areas.

The present study used the CFD method to solve the rotor's all regions. The results of the CFD method, including pressure, temperature, and velocity, are used to calculate the Gradient Length Local Knudsen. The initial evaluation for specifying the boundary of the rarefied and continuum regions is Kn<0.05 [16].

The local Knudsen number is defined by the gradient's local length of density, velocity, and temperature [17]:

$$Kn_{GLL\,\phi} = \frac{\lambda}{\phi}|\nabla\phi| = \lambda \times \left[max\left(\frac{|\nabla\rho|}{\rho}\ \frac{|\nabla V|}{V}\ \frac{|\nabla T|}{T}\right)\right] \quad (6)$$

$$\lambda = \frac{kT}{\sqrt{2}\pi D^2 p} \quad (7)$$

Where λ is the molecular mean free path, k is the Boltzmann's constant, D is the diameter of UF_6 molecules.

In the literature, the local Knudsen number ($Kn_{GLL\,\phi} = 0{,}05$) has been used to determine the interface location of the rarefied-continuum regions [15, 18, 19, 20]. The position of the boundary between the two regions was therefore predicted using the local Knudsen number.Additionally, state-based methods were used to transfer information between rarefied and continuum regions. The state-based method averages the particle information in the DSMC zone to evaluate macroscopic properties as CFD boundary conditions; meanwhile, it generates particles based on the macroscopic state of the continuum domain in DSMC buffer cells [21].

In the present hybrid algorithm, the CFD solution is not used in the near equilibrium region during the hybrid procedure. Only the NS boundary conditions are transferred into the DSMC region. This feature increases the simplicity and efficiency of hybrid simulations while the surface is calculated very accurately. Application of this method has been reported for the simulation of high-altitude plume flow [22, 23, 24].

This algorithm is considered a small overlap region at the interface between the two solvers. Both solvers are expected to result in valid solutions in the overlap region. In Fig. 1, the flowchart of the hybrid algorithm is shown. It consists of the following steps [9]:

1. Obtain an initial CFD solution for the entire domain. This solution is inaccurate in rarefied regions, but it is acceptable in the near-continuum regions.
2. Apply the breakdown parameter (Kn_{GLL}= 0.05) to the CFD solution and determine the rarefied regions.
3. Extend an overlap region in the continuum region.
4. Use the DSMC solver to obtain the solution in the rarefied and overlapped regions. Boundary conditions at the overlap region are supplied from the CFD solution.
5. Check the convergence criterion using AAE (φ)

The difference between the results is defined by the accumulated absolute error (AAE). The boundary is then extended to the continuum region to reduce the absolute error. The results are compared at an overlap outer interface between the continuum-rarefied regions. The absolute error is considered for the values of the flow properties, including temperature and velocity in the radial, angular, and axial directions.

6. If AAE (φ)>0.02, extend the overlap region inside the continuum region.
7. Go to step 4, use the previously created particles in the DSMC region at the preceding iteration and make particles in the new DSMC cells.
8. The hybrid iteration continues until the convergence parameter (AAE) indicates that the interface location does not need any more changes at the current stage.

$$AAE(\varphi)_{overlap\ outer\ boundary} = \left(\sum_{i=1}^{i=N_{cell}} \left| \frac{\varphi_{CFD} - \varphi_{DSMC}}{\varphi_{DSMC}} \right| \right) = \max \left[\left(\sum_{i=1}^{i=N_{cell}} \left| \frac{\vec{V}_{CFD} - \vec{V}_{DSMC}}{\vec{V}_{DSMC}} \right| \right), \left(\sum_{i=1}^{i=N_{cell}} \left| \frac{T_{CFD} - T_{DSMC}}{T_{DSMC}} \right| \right) \right] < 0.02 \quad (8)$$

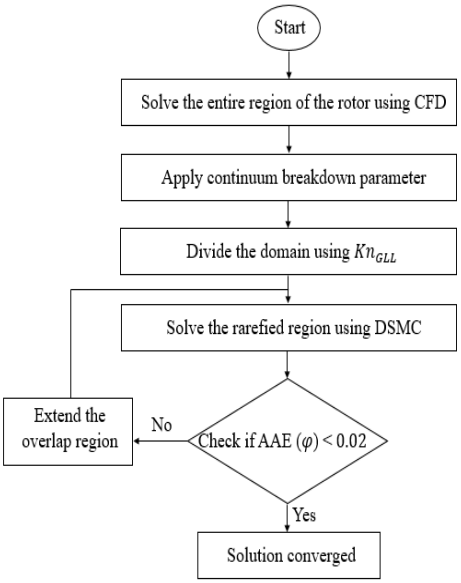

Fig. 1. Flowchart of the hybrid CFD-DSMC [9].

The size of the overlap region plays a critical role. If the size of the overlap region is small, more iterations should be performed during the procedure. However, a larger approximation for the size of the overlap region would result in more computational time for the DSMC solver in this algorithm.

In the present hybrid algorithm, we do not need to transfer any possible DSMC fluctuating solutions into the CFD region because that region is not updated during the hybrid iterations and does not require any boundary condition taken from the DSMC solution. The extracted characteristic flow obtained from the DSMC is combined only with the CFD domain. For DSMC solution, particles are created in the overlap region according to the thermal and hydrodynamic properties (temperature and velocity) obtained from CFD in the buffer region employing the Maxwellian velocity distribution.

V. Simulations

The present rotor is considered axisymmetric and steady states with a radius of 0.1 m, a length of 1 m, an angular velocity of 5500 rad/s, the cut of 0.45, and a wall temperature gradient of 20 K. The inlet mass flow rate is used to apply the inlet flow in the rotor through the feed entrance boundary. The size of the cells near the rotor wall and axis is 1.0 μm and 10 μm, respectively. Fig. 2 shows the schematic of the rotor with the location of the baffle, feed, and scoops. In addition, the structured grid inside the fluid domain is demonstrated.

The molecular weight of UF_6 is 0.352 (kg/mol), ρD is 2.306×10^{-5} (Pa.s), thermal conductivity is 0.0061 (W/m K), μ is 1.83×10^{-5} (Pa.s), Cp is 385 $(J/kg\,K)$, and diameter of UF_6 molecule is 6×10^{-10} (m) [25].

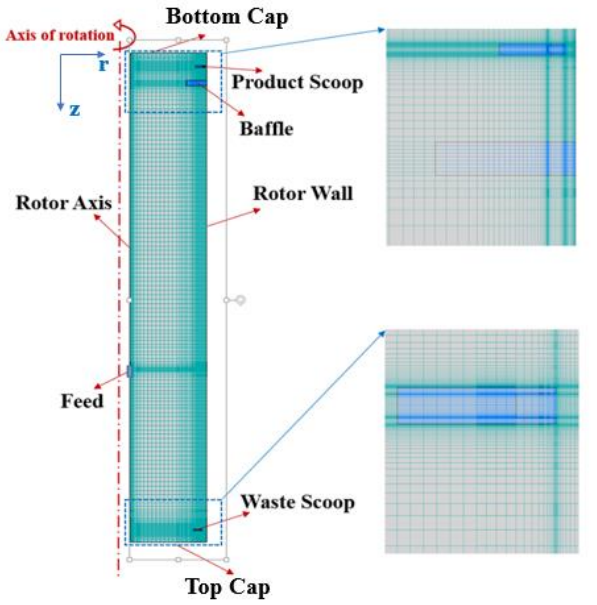

Fig. 2. Structured mesh in the fluid domain of the rotor.

VI. Results and Discussion

It is selected as the boundary between continuum and rarefied area in which the Knudsen number is 0.05 at a radius of 0.086 m. Fig. 3 shows the local Knudsen number contour calculated by CFD in the whole regions of the rotor.

As the feed plays a significant role in the gas movement inside the rotor, radial velocity distributions calculated by CFD and DSMC methods are presented in Figure. To better observe the radial velocity, this diagram is drawn in the height range from -0.1 m to 0.1 m with the radius range from 0.025 m to 0.08 m. The height of the feed injection point is considered at -0.004 m.

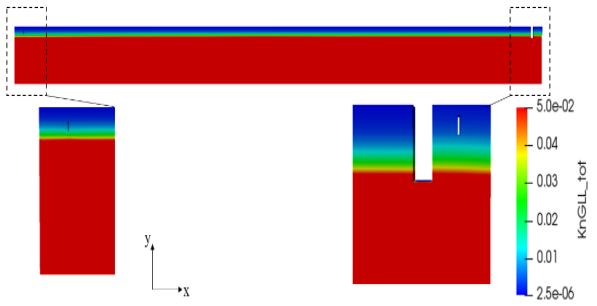

Fig. 3. The variation of local Knudsen number obtained from CFD.

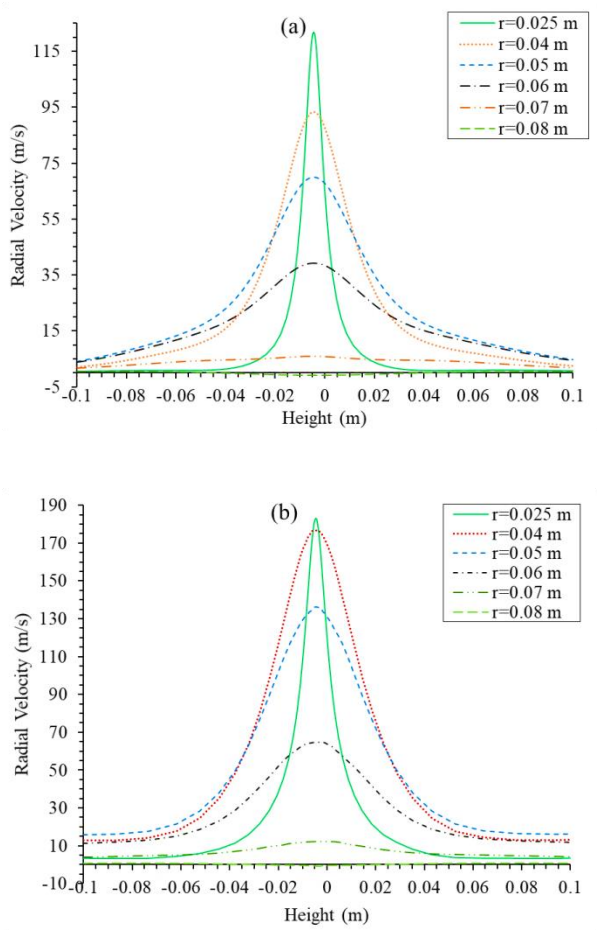

Fig. 4. The radial velocity around the feed inlet obtained from CFD (a) and DSMC (b) methods.

As can be seen, the UF_6 gas expands in front of the feed region because there is a high-pressure difference between the inlet feed and vacuum region near the axis. With the expansion of the gas, the radial velocity increases to 120 m/s and 180 m/s calculated by CFD and DSMC methods, respectively. In addition, As it moves away from the feed injection point, the radial velocity is damped so that the maximum value is the closest to the feed injection (r=0.025 m). The solution of Navier-Stokes equations using the CFD method in the rarefied zone is not sufficiently valid, so the distribution of radial velocities near the feed zone obtained from the DSMC solution is more accurate.

In Fig. 5, the axial mass flux variations in the radial direction at the mid-section of the rotor are illustrated by the two above methods. As can be seen, the results from pure CFD and CFD-DSMC methods are slightly different. But the effect of this difference on the separation performance of the gas centrifuge, which is entirely dependent on the shape and size of the axial mass flux, needs to be evaluated. To show the axial mass flux in the whole regions of the rotor, we used DSMC for the rarefied region ($0{,}02 < r < 0{,}086$) and CFD for the continuum region ($0{,}086 < r < 0{,}1$).

Using the results of the gas flow solution, the convective-diffusion equation is solved, and the concentration inside the rotor is obtained. Fig. 6 shows the axial changes of $^{235}UF_6$ gas in the axial direction obtained by the pure CFD and CFD-DSMC methods in a radius 0.096 m. As can be seen, $^{235}UF_6$ gas is enriched to about 0.0085 and depleted to about 0.006. In addition, although the difference in gas concentration distributions obtained from pure CFD and CFD-DSMC methods is slight, receiv it is needed to calculate the value of separation power obtained from the two methods for accurate evaluation.

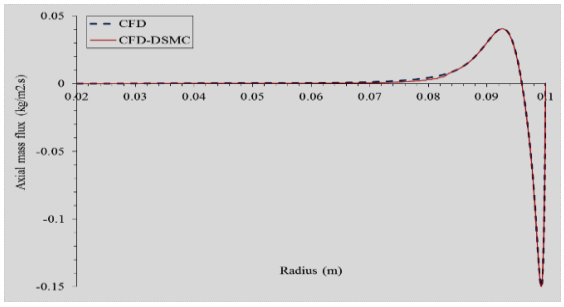

Fig. 5. Comparison of the axial mass flux variations between CFD-DSMC and CFD methods.

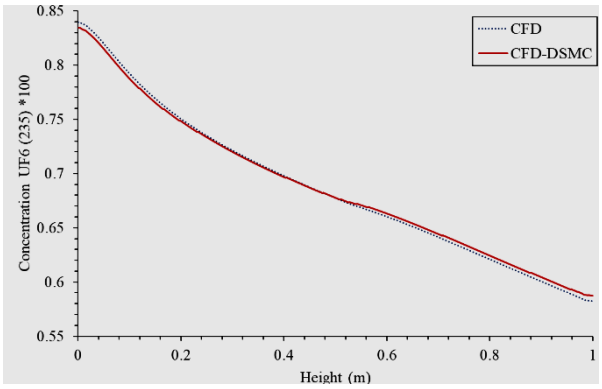

Fig. 6. Comparison of the concentration of UF_6 (235) obtained from CFD-DSMC and CFD methods.

The obtained separation power from the pure CFD and CFD-DSMC methods is 8.950 and 8.101 $Kg\ (UF_6)\ SWU/year$, respectively. Comparing the results obtained from the two methods shows about a 10.5% difference in the value of separation power. Therefore, the slight difference in the axial mass flux causes the rotor's separation parameters to change. The computational cost of CFD and DSMC methods is 24 and 50 hours, respectively (the characteristics of the computing system to perform the numerical solution are accounted for 30 cores with a processor base frequency of 2.2 GHz).

VII. Conclusions

This paper investigated the behavior of UF_6 inside a centrifuge rotor in an axisymmetric state using the CFD-DSMC method in the OpenFOAM framework. An Implicit Coupled Density-Based scheme was applied for CFD, and dsmcFoam was employed for DSMC. For simulation with CFD-DSMC, the interface location was determined at 0.086 m using the local Knudsen number. This study showed due to the invalidity of Navier-Stokes equations in the rarefied area, the results of the CFD method are different from the CFD-DSMC method. The results showed that although the CFD-DSMC method has more complexity and computational cost than the pure CFD, it is necessary to accurately and correctly evaluate the rotor separation performance, it is necessary to use the CFD-DSMC method.

References

1. J. Wu et al. *Development and verification of a coupled DSMC–NS scheme using unstructured mesh*, Journal of Computational Physics**. 219**, 579, (2006).
2. G. Abbate et al. *Coupled Navier-Stokes/DSMC method for transient and steady-state gas flows*, Springer-Verlag Berlin Heidelberg Part I, LNCS 4487, p**. 842** (2007).
3. V. Borisevich et al. *Numerical simulation of bellows effect on flow and separation*, Nuclear Instruments and Methods in Physics Research**. 455**, 487, (2000).
4. T. Kai. *Basic characteristics of centrifuges, (III) analysis of fluid flow in centrifuges*, Journal of Nuclear Science and Technology, **14**, 267, (1976).
5. D. Jiang and S. Zeng, in, *CFD simulation of 3D flowfield in a gas centrifuge*, International Conference on Nuclear Engineering (2006).
6. S. Bogovalov et al. *Verification of numerical codes for modeling of the flow and isotope separation in gas centrifuges*, Computers & Fluids. **86**, 177, (2013).
7. D. J. Jiang and S. Zeng, *"3D numerical study of a feed jet in a rotating flow-field*," International Workshop on Physical and Chemical Processes in Atomic Systems, vol. **751**, (2016).
8. V. Ghazanfari, A. Salehi, A. Keshtkar, M. Shadman and M. Askari, "*Modeling and simulation of flow and uranium isotopes separation in gas centrifuges using implicit coupled density-based solver in OpenFOAM*," European Journal of Computational Mechanics, vol. **29,** pp. 1-26, (2020).
9. V. Ghazanfari et al. *Investigation of the continuum-rarefied flow and isotope separation using a hybrid CFD-DSMC simulation for UF6 in a gas centrifuge*, Annals of Nuclear Energy. **152**, 107985, (2020).
10. M. Benedict, in: *Nuclear Chemical Engineering*, Mcgraw-Hill Book Company, (1981).
11. S. Yousefi-Nasaba et al. *Determination of momentum accommodation coefficients and velocity distribution function for Noble gas-polymeric surface interactions using molecular dynamics simulation*, Applied Surface Science. **493**, 766, (2019).
12. G. A. Bird, *Molecular gas dynamics, Oxford University Press*, London, (1976).
13. D. Boyd and T. E. Schwartzentruber, *Nonequilibrium Gas Dynamics and Molecular Simulation*, Cambridge University Press, (2017).
14. W. Wagner, *A convergence proof for Bird's Direct Simulation Monte Carlo method for the Boltzmann equation*, Journal of Statistical Physics. **66**, 1011, (1993).
15. W. Wang and I. Boyd, "Hybrid DSMC-CFD simulations of hypersonic flow over sharp and blunted bodies, in: AIAA, 36th AIAA, Thermophysics Conference, p **3644** (2003).

16. Y.-Y. Lian et al. *Improved parallelized hybrid DSMC–NS method*, Computers & Fluids. **45**, 260 (2011).

17. M. Darbandi and E. Roohi, *Applying a hybrid DSMC/Navier–Stokes frame to explore the effect of splitter catalyst plates in micro/nanopropulsion systems*, Sensors and Actuators A: Physical. **189**, 409, (2013).

18. Q. Sun, I. Boyd and G. Candler, *A hybrid continuum/particle approach for modeling subsonic rarefied gas flows*, Journal of Computational Physics. **194**, 256, (2004).

19. T. Schwartzentruber, L. Scalabrin and I. Boyd, *A modular particle-continuum numerical method for hypersonic non-equilibrium gas flows*, Journal of Computational Physics**. 225**, 1159, (2007).

20. T. Schwartzentruber, L. Scalabrin and I. Boyd, *Hybrid particle–continuum simulations of non-equilibrium hypersonic blunt-body flow fields*, Journal of Thermophysics and Heat Transfer. **22**, 29, (2008).

21. Z. Tang, B. He and G. Cai, *Investigation on a Coupled CFD/DSMC Method for Continuum-Rarefied Flows*, in: AIP Conference Proceedings; p. **535** (2012).

22. J. Papp et al. *Simulation of High-Altitude Plume Flow Fields Using a Hybrid Continuum CFD/DSMC Approach*, in: 42nd AIAA/ASME/SAE/ASEE Joint Propulsion Conference & Exhibit, , California, July 9–12, (2006).

23. S. Gimelshein et al. *Modeling of chemically reacting flows from a side jet at high altitudes*, Journal of Spacecraft and Rockets. **41**, 582 (2004).

24. R. Nanson, *Phd. thesis*, Worcester Polytechnic Institute, (2002).

25. S. Bogovalov et al. *Method of Verification of the Numerical Codes for Modeling of Flows in Gas Centrifuge*, Physics Procedia. 72, 305 (2015).

How to cite this article

V. Ghazanfari, M. M. Shadman, F. Mansourzadeh,* Investigation of Feed Flow Effect Using CFD-DSMC Method in a Gas Centrifuge, *Journal of Nuclear Science and Applications,* Vol. **2,** No. **4,** Autumn **(2022),** P **7-14,**
Url: https://jonra.nstri.ir/article_1432.html, DOI: 10.24200/jon.2022.1027